International Journal of Fracture (2006) 139:239–252
DOI 10.1007/s10704-006-0041-3

Influence of loading rate on concrete cone failure

J. OŽBOLT[1,*], K. K. RAH[1] and D. MEŠTROVIĆ[2]
[1]*Institute of Construction Materials, University of Stuttgart, 70550 Stuttgart, Germany*
[2]*Faculty of Civil Engineering Rijeka, 51000 Rijeka, Croatia*
[*]*Author for correspondence. E-mails: ozbolt@iwb.uni-stuttgart.de (Ozbolt); dmestrovic@grad.hr (Mestrovic)*

Received 6 April 2005; accepted in revised from 6 February 2006

Abstract. Three different effects control the influence of the loading rate on structural response: creep of bulk material, rate dependency of growing microcracks and structural inertia. The first effect is important only at extremely slow loading rates whereas the second and third effects dominate at higher loading rates. In the present paper, a rate sensitive model, which is based on the energy activation theory of bond rupture, and its implementation into the microplane model for concrete are discussed. It is first demonstrated that the model realistically predicts the influence of the loading rate on the uniaxial compressive behaviour of concrete. The rate sensitive microplane model is then applied in a 3D finite element analysis of the pull-out of headed stud anchors from a concrete block. In the study, the influence of the loading rate on the pull-out capacity and on the size effect is investigated. To investigate the importance of the rate of the growing microcracks and the influence of structural inertia, static and dynamic analyses were carried out. The results show that with an increase of the loading rate the pull-out resistance increases. For moderate loading rates, the rate of the microcrack growth controls the structural response and the results of static and dynamic analysis are similar. For very higher loading rates, however, the structural inertia dominates. The influence of structural inertia increases with the increase of the embedment depth. It is shown that for moderately high-loading rates the size effect becomes stronger when the loading rate increases. However, for very high-loading rate the size effect on the nominal pull-out strength vanishes and the nominal resistance increases with an increase of the embedment depth. This is due to the effect of structural inertia.

Key words: Concrete, concrete cone failure, crack band approach, finite element analysis, microplane model, rate sensitivity.

1. Introduction

It is well known that loading rate significantly influences structural response. The structural response depends on the loading rate through three different effects: (1) through the creep of the bulk material between the cracks, (2) through the rate dependency of the growing microcracks and (3) through the influence of structural inertia forces, which can significantly change the state of the stresses and strains at the material. Depending on the type of material and the loading rate, the first, second or third effect may dominate. For quasi-brittle materials, such as concrete, which exhibit cracking and damage phenomena, the first effect is important for relatively low-loading rates (creep–fracture interaction). However, the later two effects dominate for higher loading rates (impact loading). This is especially true for the case of recently observed phenomena (Bažant et al., 2000) for which a sudden increase of the loading rate in softening leads to reversal of softening into hardening.

In the literature, a number of theoretical and experimental studies can be found that deal with the problem of the rate effect for concrete like materials (Reinhardt, 1982; Curbach, 1987; CEB, 1988; Weerheijm, 1992). In most of these studies, various stress–displacement relations, similar to the spring-dashpot models of viscoelasticity, were used. In the present paper, a model for the rate dependency of the crack propagation is adopted that is applicable over many orders of magnitude of the loading rate. The model is based on the rate process theory (Krausz and Krausz, 1988) of bond ruptures. It is coupled with the M2-O microplane model for concrete (Ožbolt et al., 2001), which has been shown to realistically simulate failure of concrete structures for complex three-dimensional stress–strain states (Ožbolt, 1995).

Practical experience, a large number of experiments and numerous numerical studies for anchors of different sizes confirm that fastenings are capable of transfering a tension force into a concrete member without using reinforcement (Eligehausen et al., 1997). Provided the steel strength of the anchor is high enough, a headed stud subjected to a tensile load normally fails by cone shaped concrete breakout. Experimental and theoretical investigations clearly show that for the pull-out problem, cracking of concrete is an important aspect of the resistance mechanism. In contrast to a number of structural systems, which rely only on the material strength, the concrete cone resistance relies mainly on the energy consumption capacity of concrete, which is directly related to the concrete cracking. Since cracking is a time-dependent phenomenon, it is important to know how the loading rate influences the concrete pull-out capacity (impact, seismic action, etc.). The experimental results indicate that the loading rate significantly influence the concrete cone pull-out capacity (Klingner et al., 1998; ANCHR, 2001). However, due to the limited number of experiments, which are available only for relatively narrow range of loading rate, there is an obvious need for further theoretical and experimental investigation.

It is well known that the concrete cone resistance exhibits significant size effect on the ultimate load (Eligehausen et al., 1997). For quasi-static loading, the size effect can be well predicted by the size effect formula that is based on linear elastic fracture mechanics (LEFM) (Ožbolt, 1995). Presently there is no experimental or theoretical investigation in which the size effect on the concrete cone capacity was systematically investigated for different loading rates. For long-term loading (very low-loading rates), in which creep of concrete plays important role, the size effect becomes stronger compared to the normal loading rates (Bažant and Gettu, 1992). Therefore, one of the aims of this numerical study was to investigate how relatively fast loading rates, where creep of the concrete is of a minor importance, influence size effect on the pull-out capacity. To distinguish between the influence of the rate-dependent concrete cracking and structural inertia on the size effect, the results of static and dynamic analyses were evaluated and compared.

2. Rate dependency in the M2-O microplane model

The rate dependency in the here presented version of the thermodynamically consistent M2-O microplane model for concrete (Ožbolt et al., 2001) consists of two parts: (1) the rate dependency related to the formation (propagation) of the microcracks, which accounts for the effect of inertia forces at the level of the micro-crack tip, and (2) the rate dependency due to the creep of concrete between the microcracks. The

first part of the rate dependency is responsible for the short-duration loads (impact), up to duration of 1 h, and the second part is responsible for the long-duration loading (creep fracture interaction). Unlike the model proposed by Bažant et al. (2000), in which the initial elasticity modulus is controlled by a simple viscoelastic model, in the current model the rate dependency related to the formation of microcracks is responsible for the rate-dependent softening and for the rate-dependent hardening (rate-dependent elasticity modulus of concrete). The reason for this is due to the assumption that the microcracks start to grow immediately after the application of load. Consequently, the initial (secant) elasticity modulus is controlled by the rate of growth of microcracks. Note, that in the present formulation the influence of structural inertia on the rate effect is not a part of the constitutive law, however, this effect is automatically accounted for in dynamic analysis in which the constitutive law interacts with forces due to structural inertia.

The second part of the rate dependency, in which creep of concrete is important, is in the constitutive law represented by the serial coupling of the generalized Maxwell model for concrete and the microplane model (Ožbolt and Reinhardt, 2001). The discussion related this part of the model is out of the scope of the present paper (for more details, see Ožbolt and Reinhardt, 2001).

The rate of strain $\mathrm{d}\varepsilon/\mathrm{d}t$ in a continuum with a number of parallel cohesive cracks, which may be imagined to represent macroscopic strain softening, can be expressed as follows:

$$\frac{\mathrm{d}\varepsilon}{\mathrm{d}t}=\frac{\dot{w}}{s_{\mathrm{cr}}}+\frac{\dot{\sigma}}{E}\approx\frac{\dot{w}}{s_{\mathrm{cr}}}, \tag{1}$$

where ε = average macroscopic strain normal to the direction of parallel cracks, s_{cr} = spacing of the parallel cracks, E = Young's modulus of bulk material and $\dot{\sigma}/E$ is the elastic strain ratio which can be, compared to the crack opening ratio $\dot{w}$, neglected. After introducing a few reasonable simplifications into the concept that is based on the energy activation theory (Krausz and Krausz, 1988), the influence of the rate effect on the rate-independent stress–strain relation $\sigma^0(\varepsilon)$ can be written as:

$$\sigma\,(\varepsilon)=\sigma^{0}\,(\varepsilon)\left[1+C_2\ln\left(\frac{2\dot{\varepsilon}}{C_1}\right)\right], \tag{2}$$

where C_1 and C_2 are constants obtained by fitting test data (Bažant et al., 2000).

In the M2-O microplane model the macroscopic response is obtained by integrating normal and shear microplane stresses over all microplanes. The rate independent microplane stress components $\sigma^0_{\mathrm{M}}(\varepsilon_{\mathrm{M}})$ (M = stands for microplane volumetric, deviatoric and shear components, respectively) are calculated from the known microplane strains ε_{M} using pre-defined microplane uniaxial stress-strain constitutive relations (Ožbolt et al., 2001). It seems reasonable to assume that the rate effect on each microplane component is of the same type as given by (2). Consequently, the rate dependency for each microplane component reads (Bažant et al., 2000):

$$\sigma_{\mathrm{M}}\,(\varepsilon_{\mathrm{M}})=\sigma^{0}_{\mathrm{M}}\,(\varepsilon_{\mathrm{M}})\left[1+c_2\ln\left(\frac{2\dot{\gamma}}{c_1}\right)\right]\quad\text{with }\dot{\gamma}=\sqrt{\frac{1}{2}\dot{\varepsilon}_{ij}\dot{\varepsilon}_{ij}},\quad c_1=\frac{c_0}{s_{\mathrm{cr}}}, \tag{3}$$

where c_0 and c_2 are material rate constants, which have to be calibrated by fitting test data, $\dot{\varepsilon}_{ij}$ = components of the macroscopic strain rate tensor (indicial notation). From (3) it is obvious that the rate magnitude is not measured on the individual microplanes, which would be not objective, but on the macroscale. Furthermore, in the microplane model (3) applies on all microplane components except the volumetric compression, which is assumed to be rate insensitive. This is done because for volumetric compression there is no crack development since the material is compacted.

The above model parameters are calibrated based on the uniaxial compressive tests performed by Dilger et al. (1978). The tests have been carried out for three loading rates: $0.2\,\mathrm{s}^{-1}$, $3.33 \times 10^{-3}\,\mathrm{s}^{-1}$ and $3.33 \times 10^{-5}\,\mathrm{s}^{-1}$. Assuming average crack spacing of $s_{\mathrm{cr}} = 100\,\mathrm{mm}$, the following values are obtained from the calibration procedure follows: $c_0 = 0.0004$ and $c_2 = 0.032$. Using these parameters, the rate-dependent uniaxial compressive stress–strain curves are plotted for three different loading rates in Figure 1a. In the same figure, the test results are also plotted. Figure 1b shows the model response in the case of a sudden increase and decrease of the strain rate for the compression softening. Similar behaviour was observed in the experiments (Bažant et al., 2000). The influence of the rate effect on the uniaxal compressive strength and initial Young's modulus is shown in Figure 2. In both figures, the static strength and the static Young's modulus correspond to the strain rate of $10^{-5}\,\mathrm{s}^{-1}$ for which the average test value of the ratio between dynamic and static strengths is equal to one. As can be seen, for strain rates up to approximately $1.0\,\mathrm{s}^{-1}$ the microplane model prediction agrees well with the average trend observed in the experiments.

The rate sensitive microplane model accounts for the effect of inertia forces at the local, crack tip level, based on the energy activation theory. However, the influence of structural inertia on the rate sensitive material constitutive law is not a part of the constitutive model. This structural effect comes automatically from the structural dynamic analysis through the interaction between the inertia forces (stresses) and the constitutive law. Therefore, the above calibration of the constitutive law was carried out for moderate loading rates for which macroscopic inertia forces do not

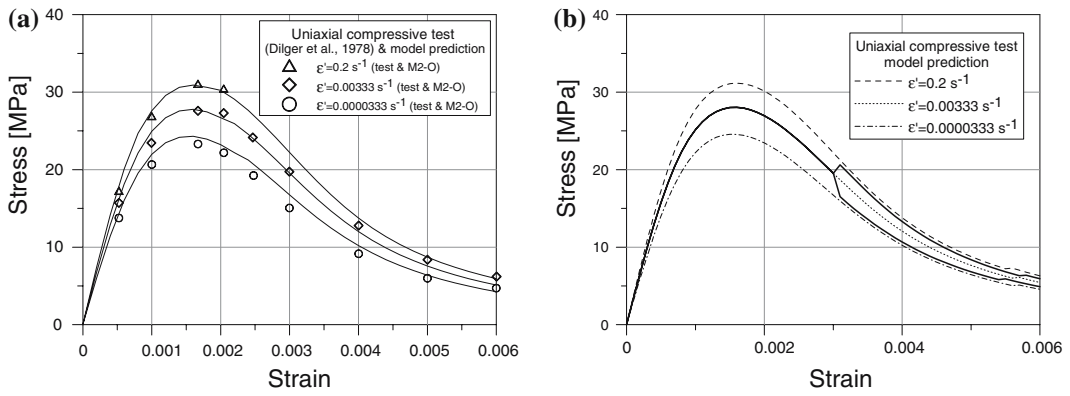

Figure 1. Uniaxial compressive test: (a) model prediction and test data (Dilger et al., 1978) and (b) model prediction – increase and decrease of the loading rate in the softening region.

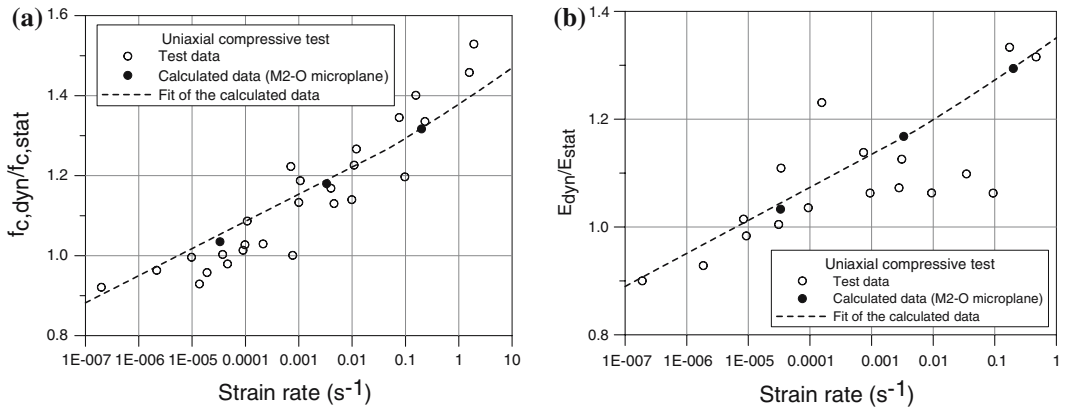

Figure 2. Uniaxial compressive test: (a) rate-dependent compressive strength – test data and model prediction and (b) rate dependent initialYoung's modulus – test data and model prediction.

have much influence on the rate dependent response of the material, i.e. only the rate of the crack growth controls the response.

The above example confirms that the presented rate sensitive microplane model is able to predict the rate sensitive response of concrete for uniaxial compression. However, in the model the rate dependency is introduced at the microplane level. Consequently, the model automatically accounts for the stress–strain-dependent rate sensitivity. This has been recently demonstrated by numerical studies in which the rate dependent response of cantilever and three-point bending plain concrete beams was studied (Ožbolt and Reinhardt, 2005a, b). Moreover, it has been shown that with the increase of the concrete quality (high-strength concrete) the influence of the loading rate decreases (Ožbolt and Reinhardt, 2005a), what is also evident from the experiments (CEB, 1988).

3. Three-dimensional FE analyses

The rate sensitive microplane model is used in the here presented 3D FE study of the pull-out problem. Static analysis is performed using an implicit 3D FE code based on the incremental secant stiffness approach (Belytschko et al., 2001). In the 3D transient dynamic FE analysis the system of unknown displacements in each time step Δt is calculated by solving the following system of equations (Voigt notation):

$$\mathbf{M}\ddot{\mathbf{u}}(t) + \mathbf{C}\dot{\mathbf{u}}(t) - \mathbf{f}(t) = 0, \tag{4}$$

where $\mathbf{M}$ = mass matrix, $\mathbf{C}$ = damping matrix, $\ddot{\mathbf{u}}$ = nodal accelerations, $\dot{\mathbf{u}}$ = nodal velocities and $\mathbf{f}(t)$ = resulting nodal forces. The resulting nodal forces are calculated as follows:

$$\mathbf{f}(t) = \mathbf{f}^{\text{ext}}(t) - \mathbf{f}^{\text{int}}(t) \tag{5}$$

with: $\mathbf{f}^{\text{ext}}(t)$ is the external nodal forces; $\mathbf{f}^{\text{int}}(t)$ is the internal nodal forces.

The above system of equations (4) is solved using an explicit direct integration scheme (Belytschko et al., 2001). The external nodal forces are known nodal loads. The internal nodal forces are unknown and they are calculated by the integration of

the stresses over the FEs. In the FE code used, the mass and damping matrices are assumed to be diagonal.

4. Influence of loading rate on concrete cone failure

The experimental results (Eibl and Keintzel, 1989; Rodrigez, 1995) for headed studs anchors loaded in tension show that the resistance and the peak displacement are higher than for the static loading. Furthermore, there is an indication that the failure mode also depends on the loading rate (Klingner et al., 1998; ANCHR, 2001). Unfortunately, the experimental results are available only for relatively low-loading rates and for anchors with relatively small embedment depths. To get more insight into the behaviour of headed stud anchors of different sizes loaded by different loading rates, a 3D static and dynamic FE analyses were carried out using the rate sensitive microplane model for concrete.

To investigate the influence of the loading rate on the concrete cone failure, pull-out of headed stud anchor from a concrete block was simulated. The edge distance was chosen such that unrestricted cone formation was possible (see Figure 3a). The heads of the studs were designed such that the pressure under the head at peak load was relatively low (approximately 3 times the uniaxial compressive strength of concrete), i.e. the heads for all embedment depths were relatively large and they were not scaled in proportion to the embedment depth. Such anchors have recently been used in the tests performed by KEPRI & KOPEC (2003) and they are often used in nuclear power plants. Three embedment depths were considered: $h_{\mathrm{ef}} = 150, 890$ and 1500 mm. In static and dynamic analyses, the load was applied by controlling

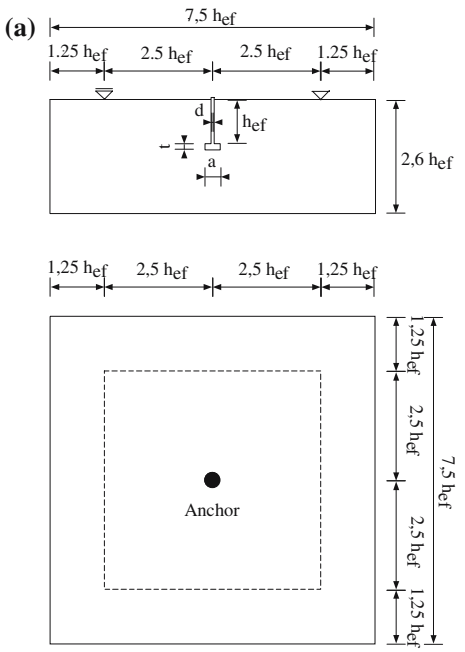

(b)

h_{ef} [mm]	d	t	a
150	16	17	40
889	95.3	102	216
1500	160.8	169	311

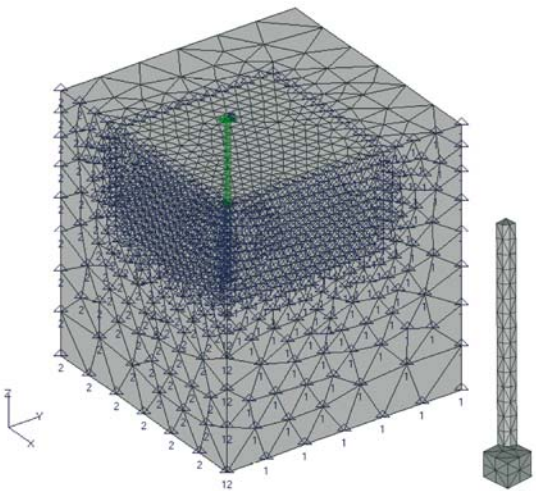

Figure 3. Investigated pull-out geometry: (a) analysis set-up and (b) geometrical data and typical finite element mesh of a concrete block and of the anchor ($h_{\mathrm{ef}} = 150$ mm, 1/4 of the specimen).

the displacement δ of the stud. This type of loading is almost identical to control of the crack opening because the anchor stud is relatively stiff and deformation of concrete under the head of the stud is relatively small (large head size). For each embedment depth the loading rates were varied from $\mathrm{d}\delta/\mathrm{d}t = 0$, (quasi-static analysis – no rate effect) to 2×10^5 mm/s. The typical finite element mesh and the geometry of the head of the stud are shown in Figure 3b. The rate independent properties of concrete are taken as: Young's modulus $E_C = 28{,}000$ MPa, Poisson's ratio $\nu_C = 0.18$, tensile strength $f_t = 3$ MPa, uniaxial compressive strength $f_c = 38$ MPa and concrete fracture energy $G_F = 0.1$ N/mm. The behaviour of steel was assumed to be linear elastic with Young's modulus $E_S = 200{,}000$ MPa and Poisson's ratio $\nu_S = 0.33$. In the analysis, four node solid finite elements were used. To eliminate mesh size sensitivity the crack band method (Bažant and Oh, 1983) was employed.

4.1. Static analysis

The typical load–displacement curves obtained in the static analysis for $h_{ef} = 150$ and 1500 mm (loading rate $\mathrm{d}\delta/\mathrm{d}t = 5$ mm/s) are shown in Figure 4. It can be seen that for the smallest embedment depth, the load–displacement curve is more ductile and, in contrast to large embedment depth, it shows two peaks. The first corresponds to the initiation of the concrete cone and the second one is due the formation of the full concrete cone. The typical load–displacement curves for all loading rates ($h_{ef} = 150$ mm) are plotted in Figure 5a. The calculated peak loads are summarised in Table 1. As can be seen, with the increase of the loading rate the peak load increases. Figure 5b shows the relative pull-out resistance for all three embedment depths as a function of the loading rate. The resistance for static loading is taken as a reference. It can be seen that for all embedment depths, the increase of the maximum pull-out resistance is almost a linear function of the loading rate (lin.-log scale). The largest increase is obtained for the smallest embedment depth. For relatively large embedment depths ($h_{ef} = 890$ and 1500 mm) the influence of the loading rate on the peak load is almost identical, however, much smaller than for $h_{ef} = 150$ mm. The reason is probably due to the fact that for small embedment depth the size of the fracture process zone is large relative to the embedment depth, which leads to a stronger

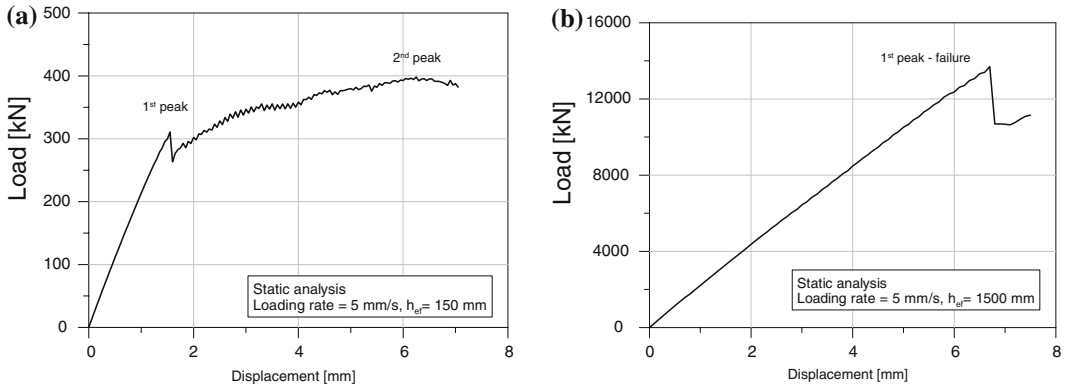

Figure 4. Static analysis – calculated load–displacement curves for: (a) $h_{ef} = 150$ mm and (b) $h_{ef} = 1500$ mm.

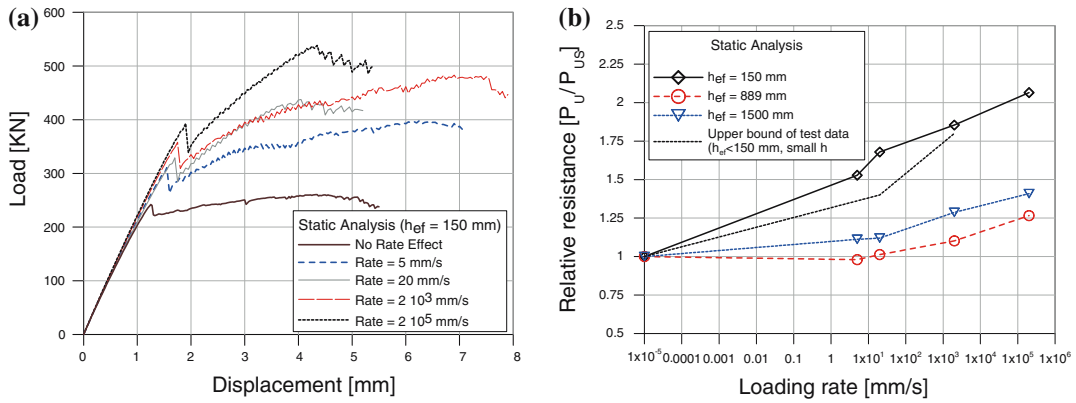

Figure 5. Static analysis: (a) calculated load–displacement curves for $h_{ef} = 150$ mm and (b) the influence of the loading rate on the anchor pull-out resistance – numerical results and upper bound of available test results (Klingner et al., 1998; ANCHR, 2001).

Table 1. Static analysis – summary of the calculated peak loads [kN].

h_{ef}[mm]	No rate effect	5 mm/s	20 mm/s	2×10^3 mm/s	2×10^5 mm/s
150	261	398	438	483	538
889	6226	6076	6304	6862	7885
1500	12,314	13,697	13,792	15,845	17,356

influence of the loading rate on the failure load. A typical concrete cone obtained in the static analysis is shown in Figure 6a. The failure mode is independent of the loading rate and of the embedment depth.

In Figure 5b is also shown upper bound of the available test data (Klingner et al., 1998; ANCHR, 2001). The tests were performed on headed stud anchors with $h_{ef} < 150$ mm and the size of the anchor heads were relatively small. In most experiments the maximal loading rate was approximately 20 mm/s (earthquake) and only few were performed with high-loading rate (ANCHR, 2001). In spite of the differences in the geometry of anchors, the numerical and experimental results show relatively good agreement. From Figure 5b it can be seen that in the experiments and in the analysis there is a similar increase of the resistance when the loading rate increases.

Numerical studies, in which the rate sensitivity was not considered, show that for anchors with relatively small head sizes the size effect is close to the prediction according to LEFM (Ožbolt et al., 2004). However, it has been recently shown (Ožbolt et al., 2004) that for larger head sizes, such as were used in the present study, the size effect obtained in experiments and in quasi-static FE analysis is weaker than the prediction based on LEFM. In Figure 6b, the relative nominal pull-out strength for all loading rates is plotted as a function of the embedment depth. For each loading rate the relative nominal strength is calculated as the ratio between the nominal strength $\sigma_N = P_U/(h_{ef}^2\pi)$ (P_U = ultimate load) and the nominal strength for $h_{ef} = 150$ mm ($\sigma_{N,150}$). The results of analysis without loading rate confirm previous results obtained by Ožbolt et al. (2004). Furthermore, it can be seen that by increase of

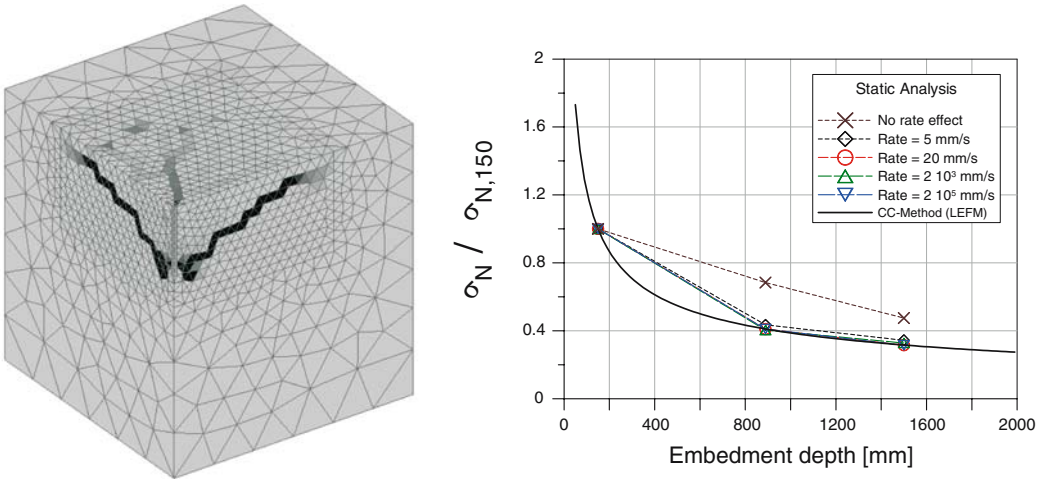

Figure 6. Static analysis: (a) Typical failure mode obtained for $h_{ef} = 150$ mm and (b) Size effect on the anchor pull-out resistance as a function of the loading rate.

the loading rate, the size effect becomes stronger, i.e. the reduction of the nominal strength for larger embedment depths is larger at higher loading rates. The results for very high-loading rates coincide almost exactly with the prediction according to LEFM.

At higher loading rates, the response is more brittle and consequently the size effect becomes stronger. This is also the case when a concrete structure is loaded slowly and the interaction between creep and fracture causes stronger size effect (Bažant and Gettu, 1992; Ožbolt and Reinhardt, 2005b). Therefore, it can be concluded that there is a transitional loading rate. For such a loading rate, the size effect is minimal. If the loading rate is larger or smaller than the transitional one, the size effect on the nominal strength increases. For slow loading rates, the creep–fracture interaction controls the rate dependency and for fast loading rates, the rate dependency is controlled by the rate-dependent crack growth. However, this holds only for moderately large loading rates for which structural inertia can be neglected.

4.2. Dynamic analysis

To investigate the influence of structural inertia on the response of the headed stud anchors, the same study as presented in Section 4.1 was repeated, however, dynamic analysis was performed. As mentioned in Section 3, dynamic analysis was carried out using an explicit direct integration method. In the analysis, damping was set to 0.023 Ns/mm. This appeared to be necessary because of numerical reasons, i.e. to get the explicit integration algorithm stable and to prevent local oscillations at the FE level. The mass density of the concrete and the anchor were set to $\rho = 2.3$ and $\rho = 7.4\,\mathrm{T/m^3}$, respectively.

The typical load–displacement curves for $h_{ef} = 150$ and 1500 mm are plotted in Figure 7 for the loading rate of 2×10^3 mm/s. For comparison, the results of static analysis are also shown. Unlike to the results of static analysis, the results of dynamic analysis for both embedment depths show relatively ductile response. It can be seen

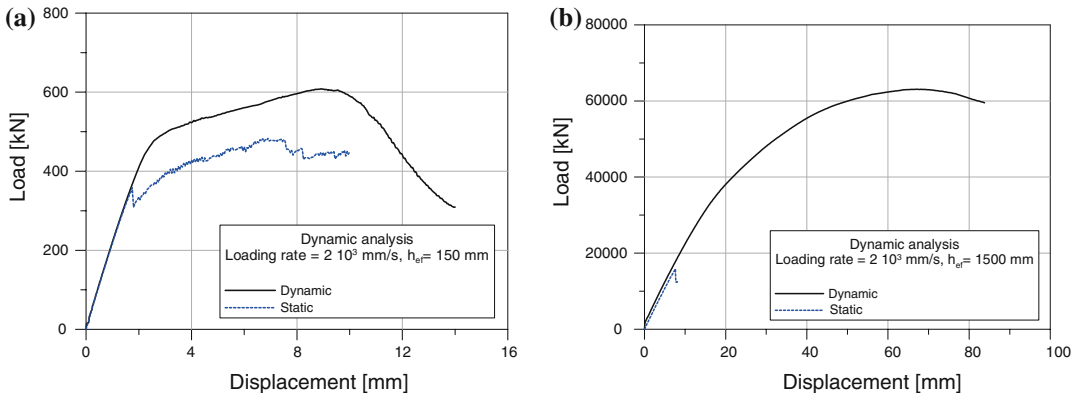

Figure 7. Dynamic and static analysis: calculated load – displacement curves for the loading rate of 2×10^3 mm/s: (a) $h_{ef} = 150$ mm and (b) $h_{ef} = 1500$ mm.

that the effect of inertia forces is much stronger in the case of larger embedment depth, i.e. compared to the static response the increase of the peak load and ductility is much higher for larger embedment depth ($h_{ef} = 1500$ mm). The peak loads for all calculated cases are summarized in Table 2. They show that similar to the static analysis, the pull-out resistance increases with an increase of the loading rate. However, for relatively high-loading rates, the increase is much higher than that in the static analysis. Moreover, it can be seen that for the same loading rate, the increase is higher for larger embedment depth. The reason for the increased strength is structural inertia forces, which are typically higher in larger structures than in small structures. The calculated load–displacement curves for $h_{ef} = 150$ mm and for three loading rates (slow, moderately fast and very fast) are plotted in Figure 8. In the figure reaction force versus prescribed anchor displacement are also shown. It can be seen that for very high-loading rates the reaction forces are not even activated at the time when the load reaches its maximum value.

The results of dynamic analysis show that the failure mode depends on the loading rate. For relatively slow loading, the failure type is the same as in the static analysis, i.e. concrete cone failure (see Figure 9a). However, for very high loading rates the failure mode changes and instead of concrete cone failure, the anchor fails in shear (mixed-mode, see Figure 9b). The same tendency was also observed in the experiments (ANCHR, 2001).

The relation between the relative maximum pull-out resistance and the loading rate is plotted in Figure 10 for all embedment depths. It can be seen that for relatively low and moderate loading rates the resistance increases almost as a linear

Table 2. Dynamic analysis - summary of the calculated peak loads [kN].

h_{ef}(mm)	No rate effect	2×10^2 mm/s	2×10^3 mm/s	2×10^4 mm/s	2×10^5 mm/s
150	261	341	608	1229	6979
889	6226	–	22, 691	73, 584	403, 000
1500	12, 314	–	63, 056	219, 204	1, 135, 280

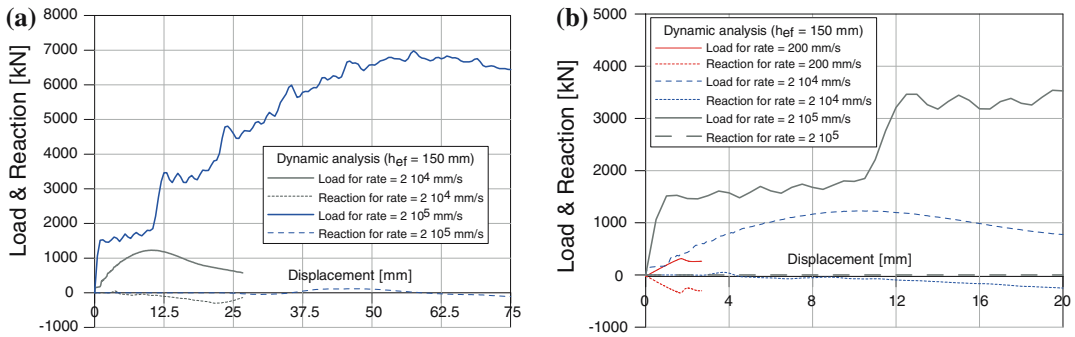

Figure 8. Dynamic analysis: calculated load (reaction) – displacement curves for $h_{ef} = 150$ mm: (a) high-loading rates up to the displacement of 75 mm and (b) detail of the displacement up to 20 mm.

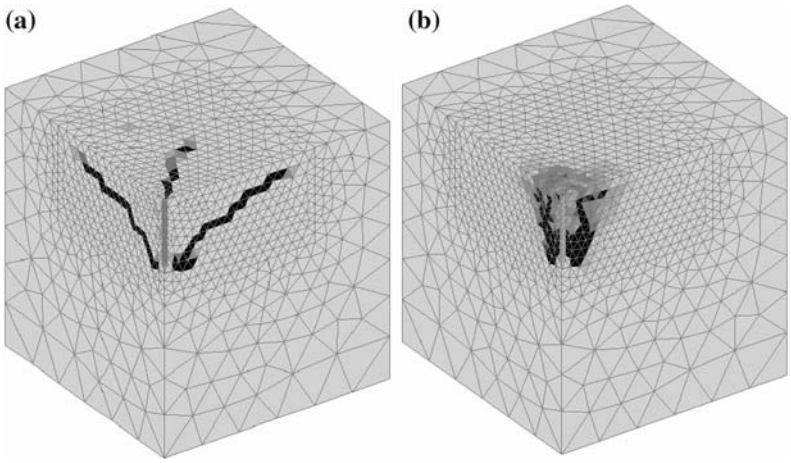

Figure 9. Dynamic analysis: calculated failure modes for $h_{ef} = 150$ mm: (a) loading rate $d\delta/dt = 200$ mm/s and (b) loading rate $d\delta/dt = 2 \times 10^5$ mm/s.

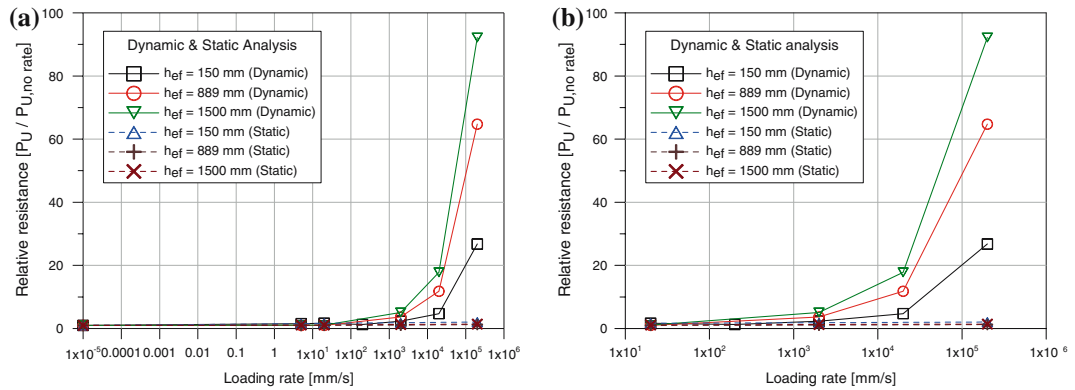

Figure 10. Dynamic analysis: influence of the loading rate on the relative pull-out resistance: (a) loading range from 10^{-5} mm/s and (b) loading range from 10 mm/s.

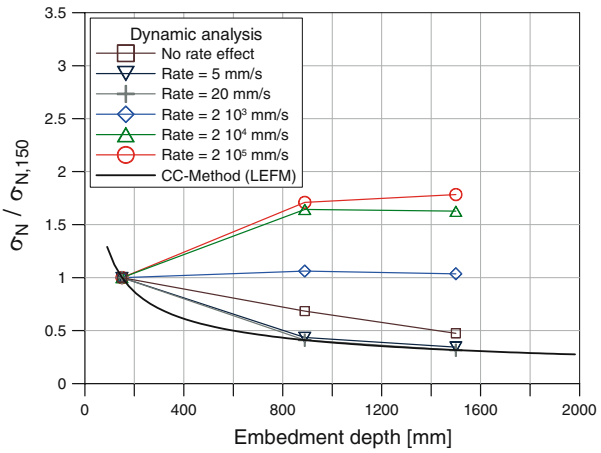

Figure 11. Size effect as a function of the loading rate (dynamic analysis).

function of the loading rate (lin.-log scale). However, after reaching certain loading rate the increase becomes progressive. The loading rate at which the resistance start to increase progressively is the critical loading rate. The critical loading rate is related to the embedment depth. The large the embedment depth, the smaller is the critical loading rate at which the increase of the pull-out resistance becomes progressive. Figure 10 shows qualitatively the same relation between the resistance and the loading rate as already observed for compressive and tensile (mode-I) rate dependent failure of concrete (CEB, 1988; Ožbolt and Reinhardt, 2005a, b).

The size effect on the nominal pull-out strength obtained in dynamic analysis is plotted in Figure 11 for all loading rates. The same as in static analysis, the relative nominal strength is shown as a function of the embedment depth. It can be seen that for moderately high loading rates the size effect becomes stronger when the loading rate increases. It reaches maximum (LEFM) for loading rates between 20 and 200 mm/s. For further increase of the loading rate, however, there is an opposite tendency, i.e. the size effect on the nominal pull-out strength is weaker. It is interesting to observe that for the loading rate $\mathrm{d}\delta/\mathrm{d}t = 2 \times 10^3$ mm/s the size effect disappears completely, i.e. the nominal pull-out strength is almost independent of the embedment depth. This loading rate approximately corresponds to the critical loading rate. For loading rates larger than 2×10^3 mm/s the nominal strength increases with the increase of the embedment depth. This is caused by structural inertia forces, which for extremely high-loading rates and large embedment depths significantly influence the pull-out resistance and failure mode.

5. Summary and conclusions

The rate sensitive model, which is based on the energy activation theory of bond rupture, is implemented into the M2-O microplane model for concrete. The comparison between model prediction and test data for uniaxial compression failure of concrete shows that the model realistically predicts the influence of the loading rate on the compressive strength and initial Young's modulus. The 3D FE static and dynamic analyses of headed stud anchors pulled out from a concrete block at various loading rates were

carried out. Based on the results of the study the following conclusions can be drawn: (1) The loading rate significantly influences the pull-out resistance of anchors. For moderately high-loading rates, static and dynamic analyses show the same response of the anchors. For these loading rates, the rate of the growing microcracks has a dominant influence on the rate-dependent response. This effect is controlled by the inertia at the local micro-crack tip level. In the constitutive model the effect is accounted for based on the energy activation theory. The comparison between experimental and numerical results shows good agreement; (2) For higher loading rates there is a large difference between static and dynamic analysis. After the loading rate reaches critical value, the increase of resistance becomes progressive. This is due to the structural inertia. At high-loading rates the influence of structural inertia on the response becomes dominant and much larger than the influence of the rate of the crack growth (constitutive law); (3) In static analysis the failure mode is typically concrete cone failure and it is independent of the loading rate. In dynamic analysis the failure mode for lower loading rates are the same as in the static analysis. However, when loading with higher loading rate the failure mode changes and is due to the shear failure (mixed-mode); (4) The results of static analysis show that the size effect on the concrete cone capacity increases with increase of the loading rate, i.e. the reduction of the nominal strength is larger if the loading rate is higher. It is known that for very low-loading rate the size effect is stronger if the loading rate is lower (creep–fracture interaction). Therefore, it can be concluded that there is a transitional loading rate for which the size effect is minimal. When the loading rate is larger or smaller than the transitional one, the size effect is stronger; (5) Dynamic analysis confirms the results of the static analysis for relatively low-loading rates. However, for higher loading rates the size effect on the nominal pull-out strength becomes weaker. For the loading rate $d\delta/dt = 2 \times 10^3$ mm/s the size effect disappears, i.e. the nominal pull-out strength becomes almost independent of the embedment depth. For loading rates higher than 2×10^3 mm/s there is an opposite tendency, i.e. the nominal strength increases with the increase of the embedment depth.

References

ANCHR (2001). *Anchorages in Normal and High Performance Concrete Subjected to Medium and High Strain Rates*. Report of the BRITE Project N^{0}BE-4199.

Bažant, Z.P. and Oh, B.H. (1983). Crack band theory for fracture of concrete. *RILEM* **93**(16), 155–177.

Bažant, Z.P. and Gettu, R. (1992). Rate effect and load relaxation in static fracture of concrete. *ACI Material Journal*, **89**, 456–468.

Bažant, Z.P., Caner, F.C., Adley, M.D. and Akers, S.A. (2000). Fracturing rate effect and creep in microplane model for dynamics. *Journal of Engineering Mechanics, ASCE*, **1126**(9), 962–970.

Belytschko T., Liu W.K. and Moran, M. (2001). *Nonlinear Finite Elements for Continua and Structures*. Wiley, New York.

Comite Euro-International Du Beton (CEB) (1988). *Concrete Structures under Impact and Impulsive Loading*. Syntesis Report, Bulletin D'Information N^0 187.

Curbach, M. (1987). *Festigkeitssteigerung von Beton bei hohen Belastungs-geschwindigkeiten*. PhD. Thesis, Karlsruhe University, Germany.

Dilger, W.H., Koch, R. and Kowalczyk, R. (1978). *Ductility of Plained and Confined Concrete under Different Strain Rates*. American Concrete Institute, Special publication, Detroit, MI, USA.

Eibel, J. and Keintzel, E. (1989). *Zur Beanspruchung von Befestigungsmitteln be dynamischen Lasten*. Forschungsbericht T2169, Institut für Massivbau und Baustofftechnologie, Universität Karlsruhe.

Eligehausen, R. Mallee, R. and Rehm, G. (1997). *Befestigungstechnik*. Ernst & Sohn, Berlin, Germany.

KEPRI and KOPEC (2003). Internal Report on: *Pre-tests for Large-sized Cast-in-place Anchors*. South Korea.

Klingner, R.E., Hallowell, J.M., Lotze, D., Park, H-G., Rodrigez, M. and Zhang, Y-G. (1998). *Anchor Bolt Behavior and Strength During Earthquakes*. NUREG/CR-5434, The University of Texas at Austin.

Krausz, A. S. and Krausz, K. (1988). *Fracture Kinetics of Crack Growth*. Kluwer, Dordrecht, The Netherlands.

Ožbolt, J. (1995). *Size Effect in Concrete and Reinforced Concrete Structures*. Postdoctoral Thesis, University of Stuttgart, Germany.

Ožbolt, J., Li, Y.-J. and Kožar, I. (2001). Microplane model for concrete with relaxed kinematic constraint. *International Journal of Solids and Structures* **38**, 2683–2711.

Ožbolt, J. and Reinhardt, H.W. (2001). Three-Dimensional Finite Element Model for Creep-Cracking Interaction of Concrete. Proceedings of the sixth International Conference CONCREEP-6, Ulm, Bažant and Wittmann, eds., 221–228.

Ožbolt, J., Eligehausen, R., Periški\'b5, G. and Mayer, U. (2004). 3D FE Analysis of Anchor Bolts with Large Embedment Depths. Proceedings of the FraMCoS-5, Willam and Billington, eds., Vail, USA, 12–16 April 2004, Vol. 2, 845–852.

Ožbolt, J. and Reinhardt, H.W. (2005a). *Dehnungsgeschwindigkeitsabhängiger Bruch eines Kragträgers aus Beton*. Bauingenieur, Springer VDI, Band 80, 283–290.

Ožbolt, J. and Reinhardt, H.W. (2005b). Rate Dependent Fracture of Notched Plain Concrete Beams. Proceedings of the 7th international conference CONCREEP-7, Pijaudier-Cabot, Gerard and Acker, eds., 57–62.

Reinhardt, H.W. (1982). Concrete under impact loading, Tensile strength and bond. *Heron* **27**(3), pp. 48.

Rodrigez, M. (1995). *Behavior of Anchors in Uncracked Concrete under Static and Dynamic Loading*. M.S. Thesis, The University of Texas at Austin.

Weerheijm, J. (1992). *Concrete Under Impact Tensile Loading and Lateral Compression.* Dissertation, TU Delft, the Netherlands.